

# Evolutionary Optimization of Layouts for High Density Free Space Optical Network Links

Steffen Limmer  
 University of Erlangen  
 Martensstr. 3  
 91058 Erlangen, Germany  
 steffen.limmer@informatik.uni-erlangen.de

Ulrich Lohmann  
 University of Hagen  
 Universitätsstr. 27/PRG  
 58097 Hagen, Germany  
 ulrich.lohmann@fernuni-hagen.de

Dietmar Fey  
 University of Erlangen  
 Martensstr. 3  
 91058 Erlangen, Germany  
 dietmar.fey@informatik.uni-erlangen.de

Jürgen Jahns  
 University of Hagen  
 Universitätsstr. 27/PRG  
 58097 Hagen, Germany  
 jahns@fernuni-hagen.de

## ABSTRACT

Electrical chip- and board-level connections are becoming more and more a bottleneck in computation. A solution to that problem could be optical connections, which allow a higher bandwidth. The usage of free space optics can avoid the problem of crosstalk and geometrical signal path crossings in systems with a high density of interconnections. The choice of appropriate design parameters, allowing the realization of such interconnections, is a complicated task. We present an evolutionary algorithm that is able to find these parameters. We describe the parallel execution of that algorithm and present optimization results.

## Categories and Subject Descriptors

G.1.6 [Mathematics of Computing]: Numerical Analysis—*Optimization*

## General Terms

Algorithms

## Keywords

optimization, evolutionary algorithm, distributed computing, PIFSO, Clos network, optical interconnect

## 1. INTRODUCTION

Optical chip- and board-level connections become more and more of interest today. In the context of a project

Permission to make digital or hard copies of all or part of this work for personal or classroom use is granted without fee provided that copies are not made or distributed for profit or commercial advantage and that copies bear this notice and the full citation on the first page. To copy otherwise, to republish, to post on servers or to redistribute to lists, requires prior specific permission and/or a fee.

GECCO'11, July 12–16, 2011, Dublin, Ireland.

Copyright 2011 ACM 978-1-4503-0557-0/11/07 ...\$10.00.

of the European Space Agency (ESA) the possibilities of replacing electrical by optical connections between connection modules in telecommunication satellites have to be observed. These connection modules represent multistage Clos networks [2]. In Figure 1 you can see the general structure of an  $n \times n$  Clos network. It consists of three stages of crossbar switches. Compared to a network consisting of only one big switch, the number of needed crosspoints is much lower.

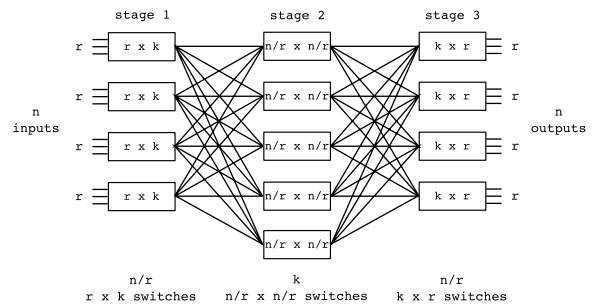
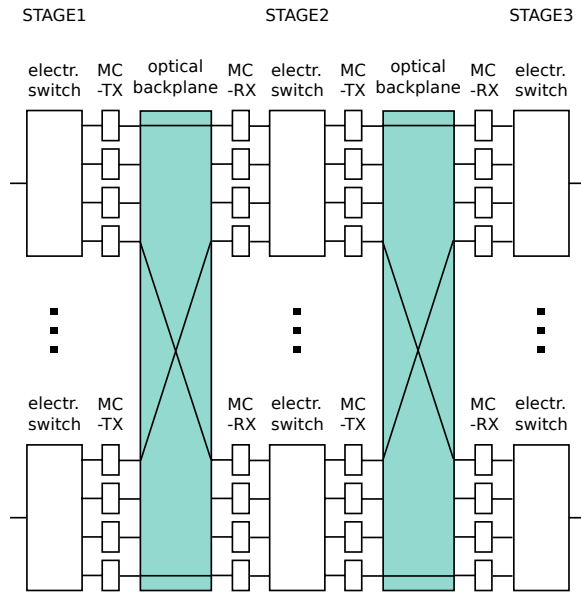


Figure 1: The general structure of a Clos network, switching  $n$  inputs to  $n$  outputs.

The Clos networks in the telecommunication satellites are currently operated with a data rate of  $300 \text{ Mb/s}$  per link [3]. The data rate shall be prospectively increased to  $3\text{-}6 \text{ Gb/s}$  per link.

For electrical distances longer than  $2 \text{ cm}$ , shifting to the optical medium seems to be a promising alternative because of rising signal degradation and increasing power dissipation of electrical interconnections compared with optical ones. Figure 2 outlines the structure of a hybrid three stage Clos network with electrical switches and an optical backplane for the interconnections of the switches. The opto-electronical media conversion is done by so called transceivers (MC-TX and MC-RX) and causes a power dissipation of about  $3\text{-}5 \text{ mW}$  per  $\text{Gb/s}$  and link. The advantages of optical links are a high bandwidth due to multiple optical channels in the same space (for example Wavelength Multiplexing) and also



**Figure 2: A three stage opto-electronical Clos network with electrical crossbar switches, an optical backplane for crossbar interconnections and MC-TX and MC-RX transceivers for the opto-electronical media conversion.**

a weight reduction compared to copper wires. A reduction in weight leads to lower fuel requirements to bring a satellite into orbit.

By the employment of free space optics the problems of crosstalk between channels and of geometrical signal path crossings can be avoided. This is especially important for higher dimensions of the network of 16 and higher. Therefore the approach of planar integrated free space optics (PIFSO) [7] together with commercially available so called MT connectors is intended for the realization. The PIFS concept is to fold a 3D optical setup into a 2D geometry in order to be compatible with planar fabrication techniques. Its advantages compared to other free space optic approaches is a high robustness as well as a good integrability and producibility, like stated out by Gruber et al [8]. A schematic illustration of a PIFS based  $4 \times 4$  network can be seen in Figure 3. The optical axis is folded into a zigzag line

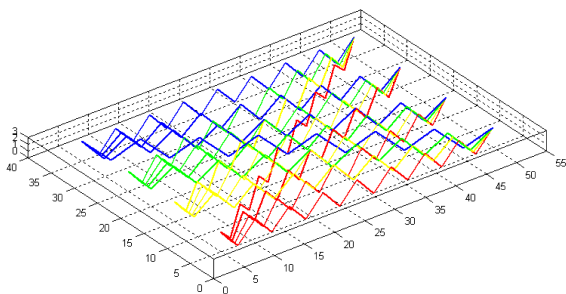


**Figure 3: A  $4 \times 4$  network in PIFS technology.**

and light propagates inside a planar substrate (for example  $\text{SiO}_2$ ) along the folded optical axis. MT connectors with

optical fibers are positioned on the surface of the substrate in order to bring the light into it and to pick the light up at the outputs. The top view on the connectors of an  $n \times n$  network with  $n=4$  can be seen in Figure 4. There are  $n$  input

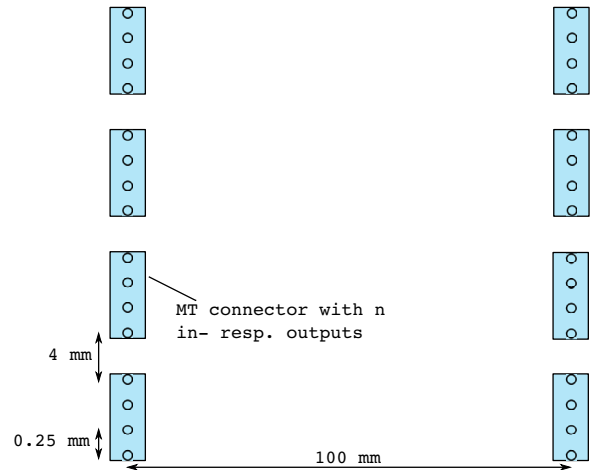


**Figure 4: The in- and output connectors of a  $4 \times 4$  network.**

and  $n$  output connectors. Each of these connectors has  $n$  fibers. The geometry of an MT connector is standardized in the IEC-61754-7 norm [1]. The pitch between two adjacent fibers of a connector is  $0.25 \text{ mm}$  and the pitch between two fibers of different connectors is at least  $4 \text{ mm}$ . The distance between two fibers in transmission direction and thus the size of the system should be limited to  $100 \text{ mm}$ .

For the realization of such a network a lot of design parameters have to be set in order to make the system meet all demands, which are described in detail in the next section. It seems to be impossible to find an optimal choice of these parameters analytically. Thus, the use of an evolutionary approach seems natural. This requires the design of a suitable fitness function and evolutionary operators. Standard operators like uniform crossover are not applicable for that problem. We present a problem-specific evolutionary algorithm (EA) that is able to find appropriate design parameters for the described optical networks.

This paper is organized as follows. In the next section the optimization problem is described. Section 3 explains the EA and Section 4 presents a distributed execution of the EA and optimization results yielded with the algorithm. Finally, Section 5 concludes, and outlines some future work.

## 2. PROBLEM DESCRIPTION

Figure 5 shows the side view of one beam in a PIFS network. The beam propagates in a certain number  $n_{FI}$  of folding intervals from the incoupling point  $A$  to the outcoupling point  $B$ . A folding interval denotes the folding of the beam by reflection with an angle  $\beta$  at the bottom of the substrate (thus, in the figure  $n_{FI}$  is two). The beams in the network have to satisfy the following three conditions:

1. The beam should hit the output as exactly as possible. This condition can be expressed by Equation 1.

$$L_{AB} = \sqrt{(\Delta x_{AB})^2 + (\Delta y_{AB})^2} \stackrel{!}{=} n_{FI} \cdot 2 \cdot \frac{H}{\tan \beta} \quad (1)$$

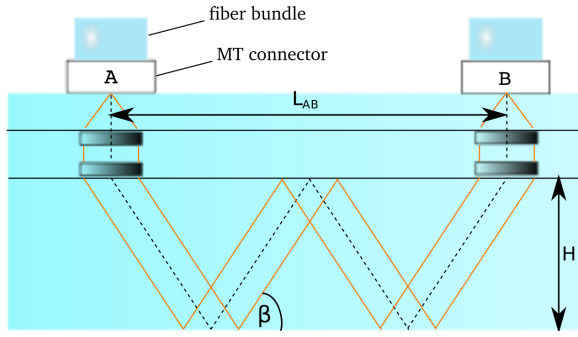


**Figure 5: Geometry of the PIFSO system.** The light paths are "folded" into the bottom substrate and propagate under an angle  $\beta$  relative to the substrate surface from an input connector A to an output connector B.  $n_{FI}$  denotes the number of double paths (also denoted here as "folding intervals").

$\Delta x_{AB}$  and  $\Delta y_{AB}$  are the distances between A and B in x- and y-direction. Thus,  $L_{AB}$  is the geometric distance between the in- and output fiber.

2. Minimize the so called skew effect as far as possible. That means that the aberrations of the optical path lengths  $L_{opt}$  of the beams from the average optical path length should be as small as possible. Thus, the transfer times of all beams are as equal as possible. This is especially important for high data rates. For example a path length difference of 10 mm in SiO<sub>2</sub> causes a signal delay of 50 ps. This is a half of the digital signal pulse width for a bandwidth of 10 Gb/s.  $L_{opt}$  can be calculated with Equation 2.

$$L_{opt} = n_{FI} \cdot 2 \cdot \frac{H}{\sin \beta} \quad (2)$$

Aberrations of more than 1 mm are not tolerable.

3. The reflection angles have to lie in the range from 32° to 43° to assure total reflection.

The angle  $\beta$  and the number of folding intervals  $n_{FI}$  can be set independently for each beam in the network. Condition 2 is the reason for the zig-zag paths of the beams. In this way it is possible to adjust the optical path lengths by an appropriate choice of the reflection angle values and the number of folding intervals.

We invented an analytical approach (described in more detail in the next section) that makes it possible to calculate the reflection angles and folding interval numbers of all beams (in the following denoted as beam parameters) for a given arrangement of the in- and output connectors, so that the first two conditions are satisfied. But with this approach the third condition is not regarded. Some of the resulting reflection angles do not lie in the desired range.

We tried to solve the task with an EA where an individual represents a setup of the folding interval numbers and angles of the beams. The fitness of an individual was calculated as the sum of the aberrations of the optical path lengths of the beams from the average optical path length. For a 4×4 network, as illustrated in Figure 4 the algorithm yielded a result with delays of the optical paths lying in a tolerable range (under 1 mm). Unfortunately this was no longer the

case for higher dimensions like 16×16 (256 beams). Here the fitness for the connector arrangement analogous to that shown in Figure 4 was 1248.08, meaning that the average aberration of the optical path length of a beam is 4.875 mm (1248.08 mm/256), which is definitely not tolerable.

But the angles and folding intervals are not the only parameters that can be set. It is also possible to change the arrangement of the connectors, thus influencing the value of  $L_{AB}$ , the geometric distance between the in- and output fiber, for a beam. We ran the EA with a lot of different arrangements of the in- and output connectors. By this way we were able to find a result with a fitness of 75.88. But the result was still not as desired. Four paths had a delay greater than 1 mm. We were not able to find better connector arrangements by hand. But it seemed possible that there exist arrangements allowing the choice of beam parameters that satisfy all the three conditions.

We designed and implemented an EA, optimizing the connector arrangement with respect to the above mentioned requirements. The next section describes this algorithm in full detail.

### 3. THE EVOLUTIONARY ALGORITHM

#### 3.1 The Individuals

An individual has to represent a possible arrangement of the in- and output connectors. A connector can be abstracted by a rectangle and so an individual can consist of a position in form of an  $(x, y)$  coordinate and a rotation angle for each connector. Thus, an individual for a 16×16 network consists of 96 real values - three values for each of the 32 connectors. Between two adjacent fibers of a connector is a pitch of 0.25 mm and each fiber has a distance of at least 2 mm to the edges of the connector. Figure 6 shows a connector to scale.

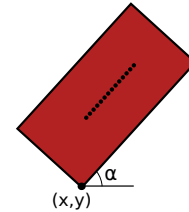


**Figure 6: A connector for a 16 × 16 network.** The connector is located at the point  $(x, y)$  and rotated by the angle  $\alpha$ .

The upper bound for the x-coordinate is 104 (mm). Thus, the maximum distance of two fibers in x-direction is 100 mm. The upper bound for the y-coordinate is 100 (mm). All the described geometrical parameters are chosen to satisfy the constraints illustrated in Figure 4.

For the evaluation of an individual, respectively a connector arrangement, we used the analytical method already mentioned in the last section. The method yields reflection angles and folding interval numbers as desired, with the exception that some of the angles may lie outside of the allowed range. Let us examine this more in detail:

Let  $n_b$  denote the total number of beams ( $n_b = n^2$  for an  $n \times n$  network). Furthermore let  $n_{FI_i}$ ,  $\beta_i$ ,  $L_{AB_i}$  and  $L_{opt_i}$  with  $0 \leq i \leq n_b - 1$  be the number of folding intervals,

the reflection angle, the distance between the in- and out-put fibers and the optical path length of the beam  $i$ . From Equation 1 it follows that for given  $n_{FI_i}$  the angles  $\beta_i$  can be calculated so that Condition 1 holds with the following formula:

$$\beta_i = \arctan\left(\frac{n_{FI_i} \cdot 2 \cdot H}{L_{AB_i}}\right) \quad (3)$$

The second condition is satisfied if all optical path lengths are equal, that means  $L_{opt_0} = L_{opt_i}$  for all  $1 \leq i \leq n_b - 1$ . Under the prerequisite that the  $\beta_i$  are set according to Formula 3 it follows from Equation 2 that this is equivalent to

$$\frac{n_{FI_i}}{\sin\left(\arctan\left(n_{FI_i} \cdot \frac{2H}{L_{AB_i}}\right)\right)} = \frac{n_{FI_0}}{\sin\left(\arctan\left(n_{FI_0} \cdot \frac{2H}{L_{AB_0}}\right)\right)}$$

This can be reformed to

$$n_{FI_i} = \frac{L_{AB_i}}{2H} \tan\left(\arccos\left(\frac{L_{AB_i} \cdot \sin\left(\arctan\left(\frac{n_{FI_0} \cdot 2H}{L_{AB_0}}\right)\right)}{2H \cdot n_{FI_0}}\right)\right) \quad (4)$$

for  $1 \leq i \leq n_b - 1$ . Thus, for a given  $n_{FI_0}$  one can calculate all other folding interval numbers according to Formula 4 and the reflection angles according to Formula 3. Since the  $n_{FI_i}$  have to be integer values, the result of Formula 4 has to be rounded. But it is possible to calculate all beam parameters in the above described way so that the position aberrations at the output fibers are zero and the delays of the optical paths are under 1 mm. However, the resulting reflection angles are not guaranteed to lie in the desired range from  $32^\circ$  to  $43^\circ$ .

Let  $B(m)$  for  $m \in \mathbb{N}$  denote the  $n_b$ -tuple  $(\beta_0, \dots, \beta_{n_b-1})$  of reflection angles, resulting from the above formulas with  $n_{FI_0} = m$ . Furthermore let  $\delta(\beta_i)$  be the aberration of the angle  $\beta_i$  from the allowed range.

*Definition 1.*

$$\delta(\beta_i) = \begin{cases} 32 - \beta_i, & \text{if } \beta_i < 32 \\ \beta_i - 43, & \text{if } \beta_i > 43 \\ 0, & \text{otherwise} \end{cases}$$

Let  $\Delta(m)$  be the sum of all  $\delta(\beta_i)$  with  $\beta_i$  in  $B(m)$ :

*Definition 2.*

$$\Delta(m) = \sum_{\beta_i \in B(m)} \delta(\beta_i)$$

That means, we are searching for a connector arrangement, for which we can find an  $m$  with  $\Delta(m)=0$ . Additionally we want the optical path length delays as small as possible. Let  $D(m)$  be the maximum of all optical path length aberrations:

*Definition 3.*

$$D(m) = \max_{0 \leq i \leq n_b-1} \left| \frac{\sum_{j=0}^{n_b-1} L_{opt_j}}{n_b} - L_{opt_i} \right|$$

with optical path lengths  $L_{opt_i}$  arising from beam parameters computed from  $n_{FI_0} = m$  like described above. Now we can define a fitness function  $f(m)$  for a value  $m$  of  $n_{FI_0}$  as follows:

*Definition 4.*

$$f(m) = \begin{cases} -\Delta(m), & \text{if } \Delta(m) > 0 \\ 100 - 100 \cdot D(m) & \text{otherwise} \end{cases}$$

For a value  $m$ , resulting in beam parameters with angles not lying in the allowed range,  $f(m)$  is negative, where  $f(m)$  is so much smaller as greater the sum of the aberrations of all angles from that range is. If all angles are lying in the desired range,  $f(m)$  depends on the aberrations of the optical path lengths from the average optical path length and lies between 0 (because the aberrations of the optical path lengths resulting from the method described above can be considered to be less than 1) and 100. The value 100 is chosen arbitrarily. The function is constructed so that the beam parameters, resulting from a certain  $m$ , are as better, as higher the function value for that  $m$  is.

To evaluate an individual,  $f(m)$  is computed for all valid values  $m$  of  $n_{FI_0}$ . These values are all those, which lead to angles  $\beta_0$  that lie in the desired range. Let  $m^{min}$  and  $m^{max}$  be the minimum and maximum value of that range. There are some values of  $n_{FI_0}$  that make the Formula 4 insolvable. That are those values where the resulting  $L_{opt_0}$  is less than the maximal  $L_{AB_i}$  (which makes it impossible to calculate all  $L_{opt_i}$  equal to  $L_{opt_0}$ ). So it may be necessary to adjust  $m^{min}$  and/or  $m^{max}$ . The fitness  $fit(I)$  of an individual is set to:

*Definition 5.*

$$fit(I) = \max_{m^{min} \leq m \leq m^{max}} f(m)$$

For  $fit$  analog observations hold like for  $f$ . An individual  $I$  with  $fit(I) = 100$  would be a "perfect" individual.

## 3.2 The Evolutionary Operators

A difficulty for the design of the EA is, that one has to make sure, that the connectors do not overlap. That has to be considered already for the random initialization of the individuals. We do the initialization in the following way: the connectors are initialized one after another and if a new initialized connector intersects with one of the previously initialized connectors, it is reinitialized until there are no more conflicts. Since in all test runs the resulting connector arrangements were constituted so that the input connectors were lying left in the allowed range (that is  $[104] \times [100]$ ) and the output connectors right or vice versa, we restricted the x-range for the initialization in the following way: all input connectors are initialized with an x-coordinate in  $[0,20]$  and all output connectors with an x-coordinate in  $[84,104]$ .

For the selection of parent individuals, tournament selection is used.

For the crossover one has to make sure that the offspring resulting from valid parent individuals (valid in the sense that there is no overlapping of connectors) are valid, too. Thus, one can not use common strategies like uniform crossover, one-point crossover or two-point crossover. The validity of the offspring is assured with the following crossover strategy. From two parent individuals, P1 and P2, two offspring O1 and O2 are generated. The connectors of an individual are numbered consecutively. There are  $2n$  connectors for an  $n \times n$  network. Let  $I.c_i$  denote the connector  $i$  of the individual  $I$ . The crossover operator first chooses a random connector  $c_j$  and sets  $O1.c_j$  to  $P1.c_j$ . If  $P1.c_j$  intersects

with some connectors  $P2.c_k$  from the second parent individual, the connectors  $O1.c_k$  are also set to  $P1.c_k$ . If these new set connectors again intersect with some other connectors  $P2.c_l$  from P2 and the connectors  $c_l$  are not already set for O1, this is repeated recursively until the new set connectors of O1 do not intersect with some other connectors from P2 that are not already set for O1. Now this is done analogously for O2.  $O2.c_j$  is set to  $P2.c_j$ . If  $P2.c_j$  intersects with some connectors  $P1.c_m$  from the first parent individual, the connectors  $O2.c_m$  are set to  $P2.c_m$  and so on. Now a connector of O1 that is unset yet, can either be chosen from P1 or from P2. In both cases it will not intersect with the previously set connectors of O1. So the first unset connector  $c_n$  of O1 is randomly chosen from P1 or from P2 and again all connectors of the other parent individual that intersect with  $c_n$  are taken recursively from the parent from which  $c_n$  was chosen. This is repeated for O1 and O2 until all connectors of them are set. Let us for example assume that the connectors of the two parent individuals P1 and P2 are arranged like shown in Figure 7. Furthermore let  $c_3$  be the

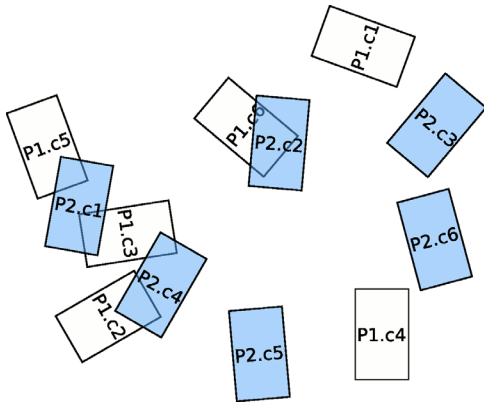


**Figure 7: Possible arrangements of the connectors of two parent individuals P1 and P2.**

first connector randomly chosen. That means  $O1.c_3$  is set to  $P1.c_3$ . This connector intersects with the connectors 1 and 4 of P2. Thus we set  $O1.c_1=P1.c_1$  and  $O1.c_4=P1.c_4$ . These connectors do not intersect with some connectors of P2, so we can proceed with O2.  $O2.c_3$  is set to  $P2.c_3$ . This does not require the setting of other connectors, since  $P2.c_3$  does not intersect with connectors from P1. The connectors of O1 are now  $(P1.c_1, -, P1.c_3, P1.c_4, -, -)$ . That means, the first unset connector is the second one. Let us choose this connector from P2 and set  $O1.c_2=P2.c_2$ . This connector intersects with  $P1.c_6$ , meaning that this connector has to be chosen from P2, too. The last unset connector of O1 is now  $c_5$ , which can be chosen for example from P1. For O2 only connector 3 is set so far and the next connector to set is number 1. If this is chosen from P2, the connectors 3 and 5 have to be chosen from P2, too (whereas connector 3 is already set). Now the connectors of O2 are  $(P2.c_1, -, P2.c_3, -, P2.c_5, -)$ . Let us choose  $c_2$  from parent 1. Then  $c_4$  has to be taken from P1, too and the last connector  $c_6$  can be chosen either from P1 or from P2. We take it from P1. Now the connectors of O1 are  $(P1.c_1, P2.c_2, P1.c_3, P1.c_4, P1.c_5, P2.c_6)$  and the connectors of O2 are  $(P2.c_1, P1.c_2, P2.c_3, P1.c_4, P2.c_5, P1.c_6)$ . These resulting offspring are illustrated in Figure 8.

The mutation of an individual is done by mutating the

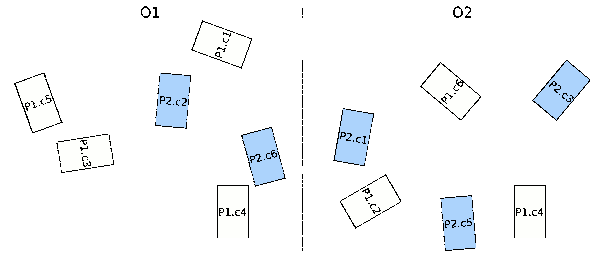


**Figure 8: Possible offspring resulting from crossover of the parents in Figure 7.**

connectors with a certain mutation probability. For the mutation of a connector, a certain number of changes are carried out. The exact number of changes is chosen randomly between one and three for each mutation. A change of a connector is either a displacement in x-direction, a displacement in y-direction, a rotation or an exchange with another connector. Exchanging connectors may appear futile at the first glance, since the complete arrangement is not changed. But an exchange will result in a new mapping of the input fibers to the output fibers, like illustrated in Figure 9. For example

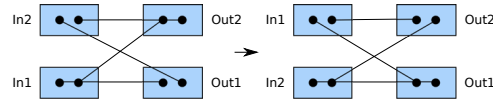


**Figure 9: The effect of exchanging two connectors. The connectors In1 and In2 are exchanged, resulting in new light channels.**

the fibers of the first input connector ( $c_1$ ) are always mapped to the first fibers of the output connectors ( $c_{n+1}, \dots, c_{2n}$ ). An exchange of the first connector with another connector will result in new light channels (in new  $LAB_i$  for some beams  $i$ ). This can lead to minor improvements. But one can assume that the potential for improvements is higher for the displacements and rotations. For this reason the probability for an exchange is set to only  $1/13$ , while the probability for each of the other changes is  $4/13$ . To keep the in- and output connectors in the x-ranges where they were initialized, as described above, the exchange is only done inside of the group of input respectively output connectors.

The displacement and rotation of a connector can not be done arbitrarily because this can lead to intersections. For this reason we compute the maximum values  $x^-$  for displacement in negative x-direction without intersection and  $x^+$  for displacement in positive x-direction without intersection. Analog values  $y^-, y^+, \alpha^-$  and  $\alpha^+$  are computed for displacement in y-direction and rotation. Figure 10 illustrates an example for these values. They have to be chosen not only depending on other connectors, but also depending on the valid ranges in x- and y-direction, to make sure, that the connector to be changed does not leave these ranges, when displaced or rotated. The displacement and rotation is done randomly with regard to the computed values.

The complete structure of the algorithm is as follows. First a population of  $p$  individuals is initialized randomly and evaluated. Then  $g$  generations are calculated. In each generation  $p$ -times crossover and mutation is done, each resulting in two offspring O1 and O2, that are evaluated. The

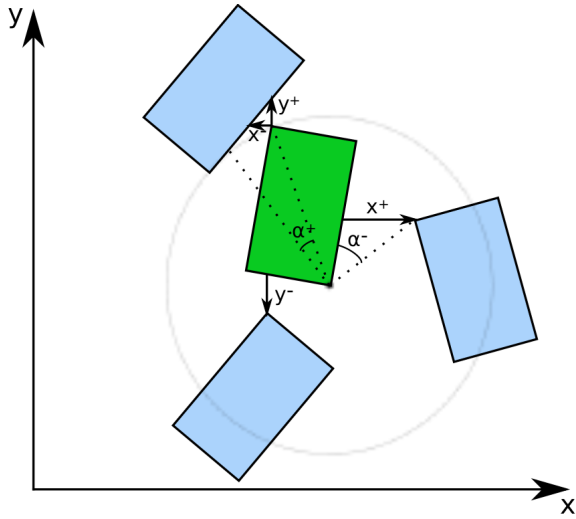


Figure 10: Clarification of the values  $x^-$ ,  $x^+$ ,  $y^-$ ,  $y^+$ ,  $\alpha^-$  and  $\alpha^+$ , that are used for the displacement and rotation of a connector.

better one of these offspring replaces the worst individual of the population, if its fitness is higher.

In the next section the obtained results of the algorithm are presented.

#### 4. RESULTS

In this section we will present the results of the optimization of a  $16 \times 16$  network with the help of the presented algorithm. Figure 11 shows the best arrangement found by hand, when searching for a skewless network with help of the EA, described in Section 2. The fitness is  $-7.83$ , meaning that for the best beam parameters several reflection angles are lying outside of the desired range and the sum of aberrations from that range is  $7.83^\circ$ . The maximum optical path length delay of this arrangement is  $0.67 \text{ mm}$ . This is the first challenge for the algorithm. It would be a success if an arrangement with a better fitness could be found.

The search space is very big. If the allowed ranges for the positions and angles would be discretized in steps of  $0.1$  (what is not done by the algorithm), the size would be about  $2.7e^{280}$ . To get an impression of the fitness landscape, we initialized one million random individuals and evaluated them. This was first done without the restriction, that the inputs have to lie “left” and the outputs “right”. The resulting individuals had an average fitness of  $-5201.70$  and the best fitness was  $-3338.58$ . With the restriction the average fitness was  $-751.93$  and the best fitness was  $-396.80$ .

Small changes on a connector arrangement can have a big impact on its fitness. You can see that the outputs in Figure 11 are a little bit displaced in  $y$ -direction, compared to the inputs. Without that displacement the fitness would decrease from  $-7.83$  to  $-34.82$ .

We ran the algorithm 20 times for a  $16 \times 16$  network. The optimizations were carried out with a population size of 1000, a crossover rate of 0.9 and a mutation rate of 0.2. 2000 generations were computed on an AMD Opteron Twelve-Core with  $2.5 \text{ GHz}$  and  $64 \text{ GB}$  RAM. In Figure 12 you can see the average evolution of the 20 runs. In two of the twenty runs a solution with all reflection angles in the al-

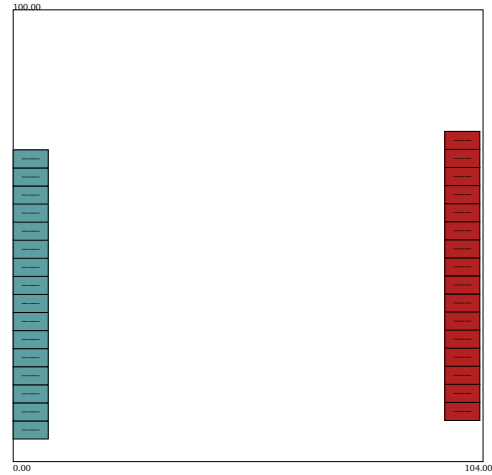


Figure 11: The best arrangement found manually. The input connectors are located at  $x=0$  and the outputs at  $x=95.55$ . The outputs are displaced by  $4.1$  in  $y$ -direction in comparison to the inputs. The fitness of this arrangement is  $-7.83$ .

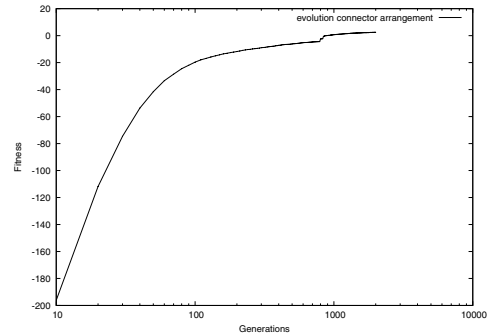


Figure 12: The average evolution of 20 runs of the algorithm with 1000 individuals, a crossover rate of 0.9 and a mutation rate of 0.2. 2000 generations were computed.

lowed range were found. The best result had a fitness of  $50.54$ , meaning that the maximum delay of the optical path lengths is  $0.495 \text{ mm}$ . The worst result of the 20 runs had a fitness of  $-9.62$ . So the algorithm is able to find connector arrangements and corresponding beam parameters with reflection angles that are completely in the desired range and additionally the path length delays could be decreased compared to the arrangement from Figure 11. The average runtime was 198 minutes.

It appears to be likely that the results can be improved by using a bigger population size and by computing more generations. But this will lead to a further increase of the already high runtime. So a parallel execution would be beneficial in this case. That is why we ran the algorithm in parallel via a self implemented framework [9], that allows the distributed execution of EAs in a grid infrastructure [6]. The distribution of the subtasks to available grid resources is done via the grid middleware Globus Toolkit [4].

For the parallelization the island model is used. The population is decomposed into multiple subpopulations on which

the algorithm is carried out simultaneously. In fixed intervals  $g$  of generations, individuals with good fitness values are migrated between the subpopulations. We use a ring topology for the migration. After the first  $g$  generations migrations take place between every population and its respective neighbor population. After further  $g$  generations there is migration to the population after next and so on, see Figure 13.

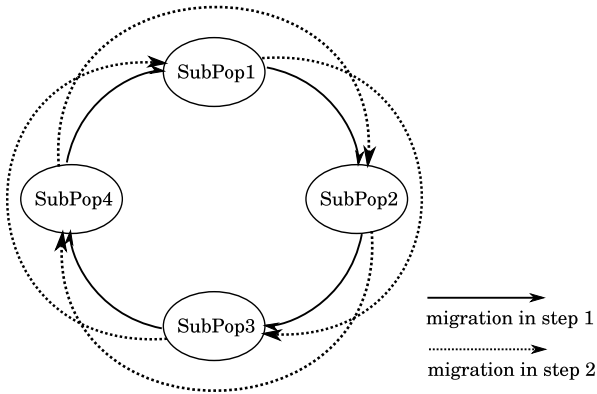


**Figure 13: Four subpopulations in ring topology. In the first migration step individuals are migrated from one subpopulation to its respective neighbor. In the second migration step individuals are migrated to the subpopulation after next and so on.**

The parallel execution in the described form will not only lead to a speedup in the runtime, but according to several papers (e.g. [5] and [10]) it can also yield a better solution quality compared to the execution without island model. The reason is a higher diversity resulting from the decomposition of the population into relatively independent subpopulations.

We ran the algorithm five times in parallel. Since the cluster of our department provides enough free resources, we did not use resources of other institutions, although it would be possible using the grid. The cluster consists of 24 machines with two AMD Opteron 2.2 *GHz* Dual-Cores each and two machines with two AMD Opteron 2.4 *GHz* Six-Cores each. The runs were done with 50 subpopulations with 1000 individuals each. 15000 generations were computed and every 300 generations migration is done. The mutation rate is 0.2 and the crossover rate 0.9, as for the serial executions.

Each of the five runs returned a result with reflection angles in the desired range. The results had an average fitness of 53.6506 and the best fitness was 55.005, meaning a maximal path length delay of 0.450 *mm*. Thus, the parallelization lead to a further improvement of the results amounting to about 10% compared to the serial execution. It is assumed that signal delays of 10% of the digital signal pulse width are acceptable. That means that the found result enables bandwidths of circa 40 *Gb/s*.

Figure 14 shows the best found connector arrangement and in Figure 15 it is shown inclusive all light beams. The average runtime of the five parallel runs was one day and 14 hours. Thus, it took about 11.5 times longer than the serial optimization, but the number of individuals was 50 times higher and the number of computed generations 7.5 times.

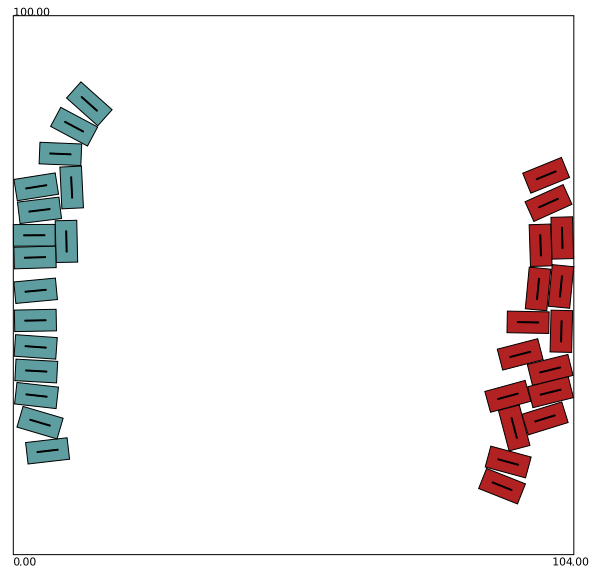


**Figure 14: The best found connector arrangement for a  $16 \times 16$  network in PIFSO technology. The maximal optical path length delay is 0.45 *mm* and all reflection angles are in the allowed range.**

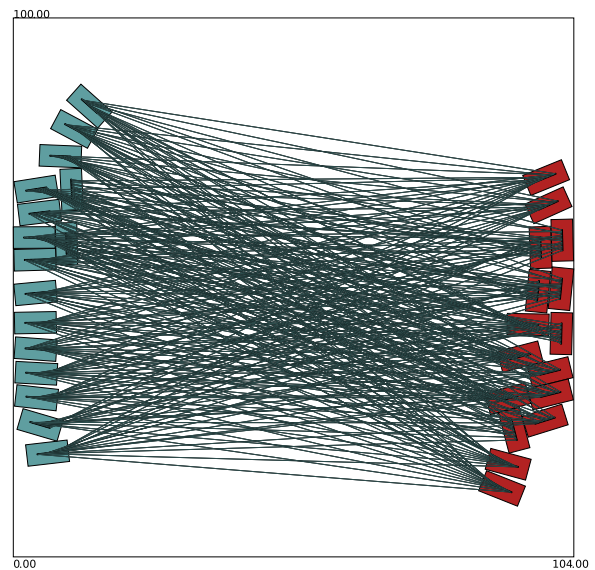


**Figure 15: The connector arrangement from Figure 14 inclusive all light paths.**

## 5. CONCLUSION

We presented an evolutionary algorithm that finally allowed us to find design parameters for free space optics based interconnections for communication networks, that can be used for the implementation. The basic approach is to optimize the arrangement of the in- and output connectors of the optical interconnections. By parallel executions in a cluster the results could be improved. We found a solution with a maximal path length delay of 0.450 *mm* which is far under the maximum acceptable delay of 1 *mm*. For the future it is planned to realize the network to gain experimental results. Furthermore we try to get comparable good

optimization results for higher dimensions than 16. Additionally it is planned to make analogous investigations for active networks, where not only the interconnections but also the switching is realized in optics by the employment of switchable mirror elements. This will lead to an additional degree of freedom for the layout.

## 6. REFERENCES

- [1] *IEC-61754-7 Norm*, 2008. Fibre Optic Interconnecting Devices and Passive Components - Fibre Optic Connector Interfaces - Part 7: Type MPO Connector Family.
- [2] C. Clos. A study of non-blocking switching networks. *Bell Sys. Tech. J.*, 32:406–424, 1953.
- [3] D. Baudet, B. Braux, O. Prieur, R. Hughes, M. Wilkinson, K. Latunde-Dada, J. Jahns, U. Lohmann, D. Fey, and N. Karafolas. Innovative on board payload optical architecture for high throughput satellites. In *Proceedings International Conference on Space Optics*, 2010.
- [4] I. Foster. A globus primer - or, everything you wanted to know about globus, but were afraid to ask. 2005. [http://www.globus.org/toolkit/docs/4.0/key/GT4\\_Primer\\_0.6.pdf](http://www.globus.org/toolkit/docs/4.0/key/GT4_Primer_0.6.pdf).
- [5] H.-M. Voigt, J. Born, and I. Santibañez-Koref. Modelling and simulation of distributed evolutionary search processes for function optimization. In *Parallel Problem Solving from Nature. LNCS*, volume 496, pages 373–380, Berlin/Heidelberg, 1991. Springer.
- [6] I. Foster and C. Kesselman. *The Grid: Blueprint for a New Computing Infrastructure*. Morgan Kaufmann, San Francisco, 1999.
- [7] J. Jahns and A. Huang. Planar integration of free-space optical components. *Applied Optics*, 28:1602–1605, 1989.
- [8] M. Gruber, J. Jahns, and S. Sinzinger. Planar-integrated optical vector-matrix multiplier. *Applied Optics*, 39:5367–5373, 2000.
- [9] S. Limmer and D. Fey. Framework for distributed evolutionary algorithms in computational grids. In *Advances in Computation and Intelligence (5th International Symposium on Advances in Computation and Intelligence), LNCS*, volume 6382, pages 170–180, Berlin / Heidelberg, 2010. Springer.
- [10] T. Starkweather, D. Whitley, and K. Mathias. Optimization using distributed genetic algorithms. In *Parallel Problem Solving from Nature. LNCS*, volume 496, pages 176–185, Berlin/Heidelberg, 1991. Springer.